

## Article

# Modeling of the Elements $\text{Ca}^{2+}$ , $\text{Mg}^{2+}$ and Si in the Sediments and the Body Walls of Sea Cucumbers in the Tropical Seagrass Meadows

Adonis Floren<sup>1,2,\*</sup>, Ken-ichi Hayashizaki<sup>3</sup>, Piyalap Tuntiprapas<sup>4</sup> and Anchana Prathep<sup>1,4,\*</sup>

<sup>1</sup> Seaweed and Seagrass Research Unit, Department of Biology, Division of Biological Science, Faculty of Science, Prince of Songkla University, Hatyai 90112, Thailand

<sup>2</sup> Institute of Environmental and Marine Sciences, Silliman University, Dumaguete City 6200, Negros Oriental, Philippines

<sup>3</sup> School of Marine Biosciences, Kitasato University, Kitasato, Minami-ku, Sagamihara 253-0373, Kanagawa, Japan

<sup>4</sup> Excellence Centre for Biodiversity of Peninsular Thailand, Faculty of Science, Prince of Songkla University, Hatyai 90112, Thailand

\* Correspondence: dnsfloren@gmail.com (A.F.); anchana.p@psu.ac.th (A.P.)

**Abstract:** The interrelationship of the minerals calcium ( $\text{Ca}^{2+}$ ), magnesium ( $\text{Mg}^{2+}$ ) and silicon (Si) in the sediments and in the body walls of four tropical sea cucumber species was explored by modeling the concentrations of these minerals. The elemental concentrations of  $\text{Ca}^{2+}$ ,  $\text{Mg}^{2+}$  and Si were measured in the body walls and in the ambient sediments occupied by the sea cucumbers *Holothuria scabra*, *H. leucospilota*, *H. atra* and *Bohadschia marmorata*. The results indicate that the concentrations of  $\text{Ca}^{2+}$  and  $\text{Mg}^{2+}$  in the body walls of the four sea cucumber species are significantly different from each other, indicating a varying degree of biomineralization across sea cucumber taxa. In contrast, only *B. marmorata* showed a significant difference in the concentration of Si when compared to the rest of the species tested. Further analysis using linear mixed models revealed that the  $\text{Ca}^{2+}$ ,  $\text{Mg}^{2+}$  and Si concentrations in the body walls of the tested sea cucumber species are associated with the sediment concentrations of the same elements. The relatively high concentrations of  $\text{Ca}^{2+}$  and  $\text{Mg}^{2+}$  in the sediments indicate that these minerals are sufficiently high in sea cucumbers to support their biomineralization. The relationship between the Mg/Ca ratio in the body walls of the sea cucumbers and minerals in the sediments revealed that Si was the only mineral that was not correlated with the Mg/Ca ratio. Predicting the relationship of the elements  $\text{Ca}^{2+}$ ,  $\text{Mg}^{2+}$  and Si between the sediments and the body walls of sea cucumbers may be complex due to the various factors that influence the metabolism and biomineralization in sea cucumbers.

**Keywords:** predictions; holothurians; biomineralization; silicon; conservation; Andaman Sea



**Citation:** Floren, A.; Hayashizaki, K.-i.; Tuntiprapas, P.; Prathep, A. Modeling of the Elements  $\text{Ca}^{2+}$ ,  $\text{Mg}^{2+}$  and Si in the Sediments and the Body Walls of Sea Cucumbers in the Tropical Seagrass Meadows. *Diversity* **2023**, *15*, 146. <https://doi.org/10.3390/d15020146>

Academic Editors: Charalampos Dimitriadis and Bert W. Hoeksema

Received: 2 October 2022

Revised: 9 January 2023

Accepted: 17 January 2023

Published: 21 January 2023



**Copyright:** © 2023 by the authors. Licensee MDPI, Basel, Switzerland. This article is an open access article distributed under the terms and conditions of the Creative Commons Attribution (CC BY) license (<https://creativecommons.org/licenses/by/4.0/>).

## 1. Introduction

Sea cucumbers are traded globally for their prized body walls, which possess good nutritional and medicinal properties. The body wall or integument of sea cucumbers is the most developed among the echinoderms, and the calcareous skeleton has been reduced to microscopic ossicles [1]. Generally, it occupies approximately 54% of the wet weight of sea cucumbers [2] and has a high regenerative capacity [3]. Additionally, the body wall also rapidly changes its mechanical properties as the calcium concentration has a profound effect on the stiffening or softening of this tissue [4,5]. However, cations other than calcium also affect the mechanical properties of the isolated catch connective tissues [6]. For example, a high magnesium concentration in the dermis of *H. leucospilota* results in high viscosity, although the results are controversial due to the high concentrations used in experimental treatments [7]. On the other hand, magnesium ions act as calcium carbonate nucleators in addition to constraining the growth of crystals and determining the crystallographic

orientation of the skeleton [8,9]. Moreover, calcium is known to be a messenger in the signal transduction process. It is also required for neurotransmission, muscle contraction and blood coagulation [10]. Thus, there is an inherent overlapping function of  $\text{Ca}^{2+}$  for metabolism, soft tissue growth and calcification [9,10].

In contrast to calcium and magnesium, relatively little is known about silicon despite its abundance in nature and the various functions it plays for support, protection [11–13] and the uptake of  $\text{Ca}^{2+}$  and  $\text{Mg}^{2+}$  [14]. In fact, the presence of Si in the tissues of sea cucumbers was only documented in the dermal granules of the deep-water species *Molpadia intermedia* [15]. This was contrasted by calcium and magnesium which were documented in numerous echinoderm taxa [16,17]. Additionally, silicon is rarely found in its elemental form due to its great affinity for oxygen, with which it binds to form silica and silicates [13,18]. Although this mineral is highly stable, chemical and biological weathering releases silicon from these stable compounds in the form of weak silicic acid [13,14]. In fact, the essentiality of Si to animal nutrition is connected to its concentration in animal tissue concentrations, reflecting the number of biochemical processes it is part of [14]. However, the excessive accumulation of this mineral may also lead to the overstimulation of fibroblast cells, resulting in the production of excess collagen that may affect biomineralization. Thus, it has been suggested that a controlled deposition of silicon is required, whether the mineral plays structural roles or the mineralization process is used as a mechanism to dispose excess silicon [19]. This suggestion is in line with the idea that eutrophication in seawater can lead to an increased accumulation of biogenic silica in the sediments brought about by increased diatom biomass production [20].

The majority of the research conducted on biomineralization has focused on organisms that are highly calcified, and on its biochemical composition once embedded in the skeleton and not necessarily in its mineral form at the time of formation [21]. Consequently, there has been considerable progress in documenting the cellular composition of the enveloping soft tissue to understand the mechanism of calcite secretion in the larvae of echinoderms [22]. However, recent studies suggest that sea cucumbers are effective at dissolving inorganic carbon by the ingestion of sands [23,24] and in the uptake of organic carbon and nitrogen from the sediments [25]. It is for this reason that the mineral concentration in the body walls of sea cucumbers must be examined in detail by determining a relationship between the minerals obtained from the sediments and those present in the body walls of sea cucumbers. As Yuan et al. [26] highlighted, little has been undertaken to understand the accumulation of minerals by sea cucumbers, which are less reliant on calcification [26]. Thus, the significant interaction between sediment-bound metals and sediment-ingesting sea cucumbers remains to be elucidated in the research in more detail [27].

In this study, we determine the mineral concentrations of  $\text{Ca}^{2+}$ ,  $\text{Mg}^{2+}$  and Si in the sediments and body walls of four sea cucumber species, *H. scabra*, *H. atra*, *H. leucospilota* and *Bohadschia marmorata*, found in the seagrass meadows of the southwestern Andaman coast. The variation in the degree of calcification of each sea cucumber species was used to explain the different mechanisms as sea cucumbers respond to changes in the mineralogy of the sediments. However, the relationship of the minerals  $\text{Ca}^{2+}$ ,  $\text{Mg}^{2+}$  and Si between the sediments and body walls of the sea cucumbers is unclear, since the principal route of  $\text{Ca}^{2+}$  uptake for larval echinoderms is often understood to be sourced from the seawater [28,29]). A recent study suggests the importance of the diet in determining sea urchin size irrespective of the  $\text{pCO}_2$  level, and the relevance of the macroalgal diet in modulating the urchin Mg/Ca ratio [30]. It was subsequently demonstrated that lowering the Mg/Ca ratio in the seawater and enriching the diet with  $\text{Mg}^{2+}$  had significantly increased the  $\text{Mg}^{2+}$  content of the sea urchin's skeletons [31]. Thus, a good understanding of the sediment mineralogy that affects biomineralization in adult sea cucumbers is crucial for the management of sea cucumbers, which are dependent on the healthy seagrass meadow as a habitat and food source (i.e., [25,32,33]).

## 2. Materials and Methods

### 2.1. Study Sites

Sea cucumbers and sediment samples were collected from the intertidal areas in the four seagrass meadows of southwest Thailand, namely, Talibong Island, Muk Island, Lidee Island and Phuket Island (Figure 1). The seagrass in Talibong Island forms an extensive meadow covering an area between 24 to 61 km<sup>2</sup>, which varied due to the seasonal run-offs from the Trang River [34]. The study site was mostly dominated by *Enhalus acoroides* and *Thalassia hemprichii* in the intertidal area, while the subtidal zone was mostly occupied by *Halophila ovalis* [35]. The seagrass meadow of Muk Island is small with an area of <1 km<sup>2</sup> and is located adjacent to the large meadow of Laem Yong Lam with an area of 18 km<sup>2</sup>, which is mostly dominated by the seagrass *Enhalus acoroides*, followed by *Halophila ovalis* and *Thalassia hemprichii* [36]. Lidee Island, on the other hand, is located in Satun Province, approximately 100 km south of the Talibong and Muk Islands. The seagrasses of Lidee are sparse and composed of *H. ovalis* and *T. hemprichii*, which are mainly found on the edges of macroalga *Halimeda macroloba* beds. In Tang Ken Bay, Phuket Island, the seagrass bed is located adjacent to the thriving coral reefs so that the sea cucumbers *B. marmorata* potentially transit across the landscape, as observed during this study. In contrast, the populations of *H. scabra* were mainly found in the seagrass meadows, while *H. leucospilota* and *H. atra* were commonly found to be associated with the *H. macroloba* beds and/or with sparse seagrass beds [37].

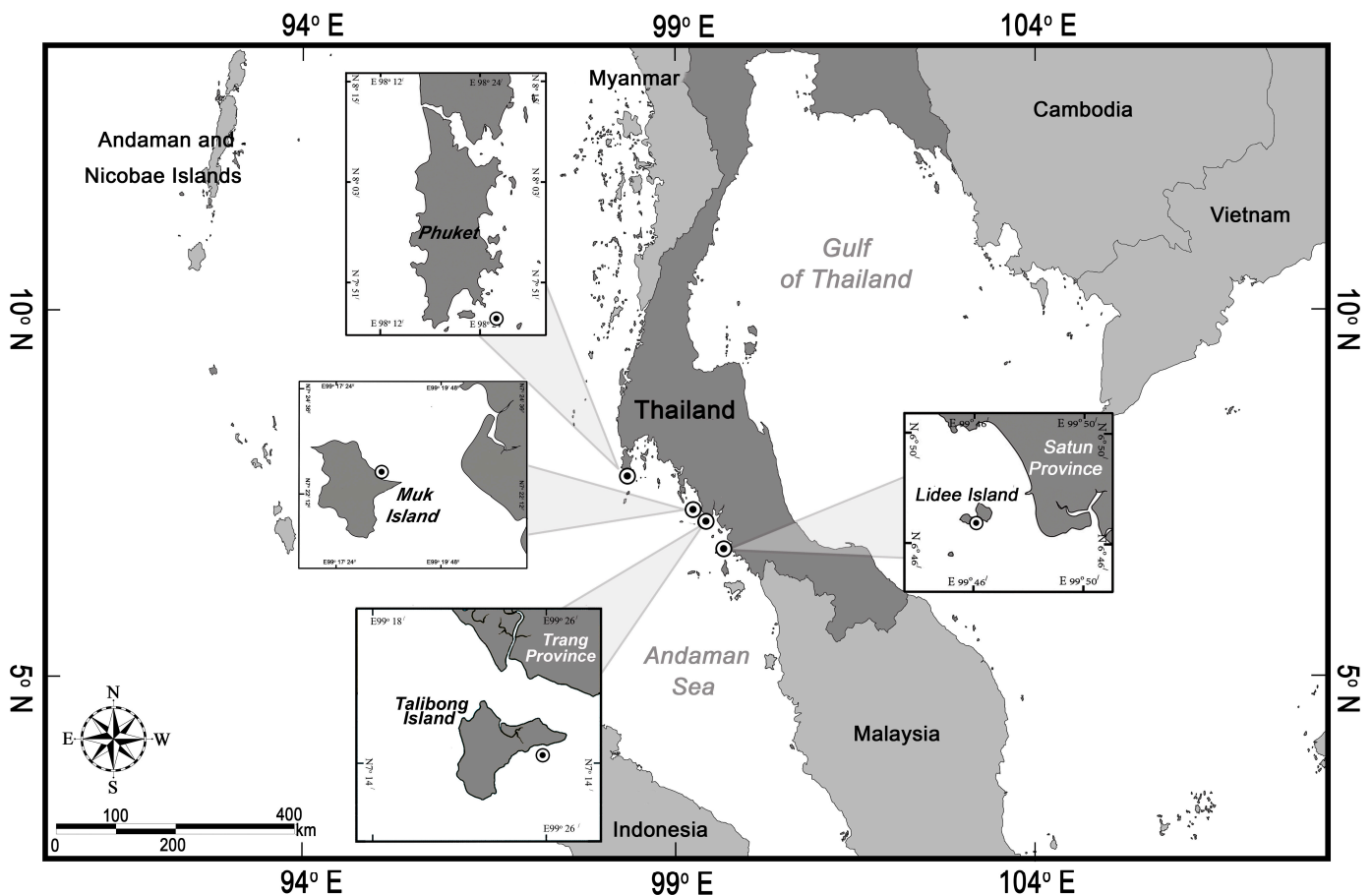


**Figure 1.** Map of southwest Andaman coast, Thailand, where the sea cucumbers and sediments were collected.

### 2.2. Sampling and Processing of Samples

Sea cucumbers and sediments were collected by hand during a low tide in each meadow in January, February, March and April 2018, and January 2019. Surface sediment

(<1 cm) samples were collected within a 1–3 m vicinity around each sea cucumber. The sea cucumbers were transferred to plastic boxes containing seawater, where the sea cucumbers were allowed to remove their excreta in the field site for 8–12 h. The seawater in the plastic box was exchanged with clean, fresh seawater 2–4 times. The sea cucumbers were then anesthetized in ice water and later stored in a freezer at  $-20\text{ }^{\circ}\text{C}$  until processing.

In the laboratory, the sea cucumber samples were thawed, and their internal organs were removed and rinsed with Milli-Q water (Millipore). The inorganic ossicles and organic soft tissue were not separated since the present study focused on determining the overall response of the sea cucumbers to changes in mineral concentrations in the sediments from a certain habitat. The sea cucumbers' body walls and sediments were then freeze-dried to a constant dry weight. The samples were ground to a fine powder using a mortar and pestle prior to measuring the concentrations of  $\text{Ca}^{2+}$ ,  $\text{Mg}^{2+}$  and Si in the samples.

Sediment and sea cucumber samples, each weighing 0.05 g, were digested with 10 and 2 mL of 65%  $\text{HNO}_3$  (Merck, p.a), respectively, following a method modified from [38]. The acid digestion was performed for 1.5 h in a  $90\text{ }^{\circ}\text{C}$  water bath. Hydrogen peroxide ( $\text{H}_2\text{O}_2$ ) was added to the solution and heated in a water bath at  $90\text{ }^{\circ}\text{C}$  for another 30 min. Digests of sediment and body wall samples were then diluted to 20 mL with Milli-Q water (Millipore) and filtered using Whatman No. 1 filter paper.

The metal concentrations of the samples were measured using PerkinElmer Avio 500 ICP-OES using the AOAC 2019 manual [39]. The wavelengths for the metal readings were 315.887 nm for  $\text{Ca}^{2+}$ , 285.213 nm for  $\text{Mg}^{2+}$  and 251.611 nm for Si. The concentration values for the sea cucumber and sediment were expressed in mg/g dry weight. The standard reference material (SRM) used to test the accuracy and precisions of the device and calibration curve was initially analyzed and then, after the analysis of each sample, in triplicate [39]. In this study, standard solutions supplied for determining the metal concentrations ( $\text{mg g}^{-1}$  dry wt.) for the sediment samples were certified reference materials of PerkinElmer Pure.

### 2.3. Statistical Analysis

The statistical analysis in this study was performed with R program version 4.0.4 [40]. The Kruskal–Wallis test was used to identify significant differences in the sea cucumber body wall tissue's and sediment's elements among the species of sea cucumbers and sites by using the R package companion [41]. Pairwise comparisons were used to compare each factor by using the Wilcoxon rank sum test, which was performed with the FSA package [42]. Generalized linear mixed models (GLMMs) with the MASS [43], lme4 [44] and tidyverse packages were used to determine the effect of the elements in the environmental sediment on the elements in the sea cucumber tissue by using the location as the random effect in the model, where the Laplace approximation was used to estimate the significance of the parameters in the model. Then, the full model for *H. scabra* and *H. atra-leucospilota* followed the form of element  $a$  in the tissue = element  $a$  in sediment + element  $b$  in sediment + element  $c$  in sediment + element  $d$  in sediment + random effect ( $1 \mid \text{Location}$ ), where  $a$ ,  $b$ ,  $c$  and  $d$  represent  $\text{Ca}^{2+}$ ,  $\text{Mg}^{2+}$ , Si and  $\text{Mg}/\text{Ca}$ , respectively. However, the generalized linear model (GLM) was used to analyze for *B. marmorata*, which was found only in one location and with no random effect. The distribution of the parameter in the model was assumed to be a gamma distribution, and the link function was a log function. Additionally, the values obtained for *H. atra* and *H. leucospilota* were pooled together and referred to as *H. atra-leucospilota* considering the close similarity in gross morphology and the limited number of samples that could be collected due to availability and permit restrictions.

## 3. Results

### 3.1. Comparison among Species and Locations

The Kruskal–Wallis rank sum test showed that the mineral concentrations (i.e.,  $\text{Ca}^{2+}$ ,  $\text{Mg}^{2+}$ , Si and  $\text{Mg}/\text{Ca}$  ratios) in the body walls of the sea cucumbers *H. scabra*, *H. atra*,

*H. leucospilota* and *B. marmorata* significantly varied among the four species (Table 1). Pairwise comparisons using Wilcoxon rank sum test revealed significant differences in the mineral concentrations in the body walls of the sea cucumbers, which varied according to the following patterns: (1)  $\text{Ca}^{2+}$ : *B. marmorata* > *H. scabra* > *H. leucospilota* > *H. atra*, (2)  $\text{Mg}^{2+}$ : *H. scabra* = *B. marmorata* > *H. atra* > *H. leucospilota*, (3) Si: *H. atra* = *H. leucospilota* = *H. scabra* > *B. marmorata* and (4) Mg/Ca: *H. atra* = *H. leucospilota* > *H. scabra* > *B. marmorata*. The same test also revealed significant differences in the concentrations of minerals in the sediments occupied by the sea cucumbers, which varied according to the following patterns: (1)  $\text{Ca}^{2+}$ : Phuket > Lidee > Muk > Talibong, (2)  $\text{Mg}^{2+}$ : Lidee > Talibong > Muk, (3) Si: Talibong = Lidee = Phuket = Muk and (4) Mg/Ca = Talibong > Muk > Lidee = Phuket. However, there was no significant difference in the concentration of Si in the sediments across the sampling sites, indicating the abundance of this mineral in the sediments. Further testing on the possibility of contamination of the samples by the reagents (i.e.,  $\text{HNO}_3$ ,  $\text{H}_2\text{O}_2$ ) that were used in the digestion of the samples showed that these reagents had Si concentrations of  $0.056 \pm 0.0036$  mg /L (mean  $\pm$  sd; n = 3) which were lower than the sea cucumber and sediment sample values of  $0.337 \pm 0.160$  mg /L (mean  $\pm$  sd; n = 3). This shows that the Si values recorded for the sea cucumbers and sediments were above the detection limit of the machine.

**Table 1.** The mean  $\pm$  SE concentration (mg/g dry weight) of the elements  $\text{Ca}^{2+}$ ,  $\text{Mg}^{2+}$  and Si for the sea cucumbers *H. scabra* (Hs), *H. leucospilota* (Hl), *H. atra* (Ha) and *B. marmorata* (Bm) collected from the Islands of Talibong, Muk, Phuket and Lidee.

| Element (mg/g DW) | Sample   | Talibong           |                   | Muk               |                   | Phuket             | Lidee             | Differences among Species<br>Kruskal-Wallis (Chi-Squared) |
|-------------------|----------|--------------------|-------------------|-------------------|-------------------|--------------------|-------------------|---|
|                   |          | Hs (n = 24)        | Hl (n = 24)       | Hs (n = 45)       | Ha (n = 15)       | Bm (n = 9)         | Ha (n = 18)       |   |
| $\text{Ca}^{2+}$  | Tissue   | 129.35 $\pm$ 18.44 | 18.83 $\pm$ 0.71  | 69.20 $\pm$ 4.20  | 12.79 $\pm$ 0.95  | 170.89 $\pm$ 14.78 | 24.67 $\pm$ 6.51  | 92.24 **  |
|                   | Sediment | 6.62 $\pm$ 0.90    | 5.56 $\pm$ 0.32   | 15.28 $\pm$ 0.68  | 11.62 $\pm$ 1.33  | 285.14 $\pm$ 5.42  | 258.29 $\pm$ 2.97 | 64.24 **  |
| $\text{Mg}^{2+}$  | Tissue   | 18.59 $\pm$ 1.16   | 9.54 $\pm$ 0.25   | 17.41 $\pm$ 0.27  | 10.84 $\pm$ 0.29  | 16.38 $\pm$ 0.61   | 9.90 $\pm$ 0.34   | 99.60 **  |
|                   | Sediment | 2.82 $\pm$ 0.15    | 3.00 $\pm$ 0.15   | 2.25 $\pm$ 0.10   | 1.68 $\pm$ 0.06   | 7.44 $\pm$ 0.17    | 7.36 $\pm$ 0.09   | 28.64 **  |
| Si                | Tissue   | 0.048 $\pm$ 0.004  | 0.043 $\pm$ 0.003 | 0.042 $\pm$ 0.003 | 0.025 $\pm$ 0.001 | 0.019 $\pm$ 0.000  | 0.081 $\pm$ 0.013 | 22.59 **  |
|                   | Sediment | 0.074 $\pm$ 0.003  | 0.080 $\pm$ 0.002 | 0.084 $\pm$ 0.003 | 0.071 $\pm$ 0.002 | 0.081 $\pm$ 0.001  | 0.089 $\pm$ 0.004 | 0.49 ns   |
| Mg/Ca             | Tissue   | 0.187 $\pm$ 0.014  | 0.516 $\pm$ 0.015 | 0.281 $\pm$ 0.012 | 0.899 $\pm$ 0.055 | 0.099 $\pm$ 0.005  | 0.723 $\pm$ 0.093 | 92.69 **  |
|                   | Sediment | 0.644 $\pm$ 0.076  | 0.596 $\pm$ 0.048 | 0.155 $\pm$ 0.007 | 0.170 $\pm$ 0.016 | 0.026 $\pm$ 0.001  | 0.029 $\pm$ 0.000 | 69.80 **  |

When \*\* =  $p < 0.001$ , ns = not significant, the number of sea cucumber samples was shown as n = in the parentheses.

### 3.2. Relationship between Tissue $\text{Ca}^{2+}$ and Sediment $\text{Ca}^{2+}$ , $\text{Mg}^{2+}$ and Si

The GLMM revealed that only the  $\text{Ca}^{2+}$  in the ambient sediment was a significant predictor for the  $\text{Ca}^{2+}$  in the body walls of *H. scabra* and *H. atra-leucospilota*, since the slopes of the models (log-scale) were  $-0.06 \pm 0.01$  and  $-0.05 \pm 0.01$  (mean  $\pm$  SE;  $t$ -value =  $-7.50$  and  $-6.50$ ;  $p$ -value < 0.01; Figure 2) and the intercept values were  $5.25 \pm 0.24$  and  $7.12 \pm 3.30$  ( $t$ -value = 22.00 and 2.16;  $p$ -value < 0.001 and 0.03), respectively. For *B. marmorata*, the GLMM showed that the  $\text{Ca}^{2+}$  concentrations in the body walls could also be predicted by the  $\text{Ca}^{2+}$  and  $\text{Mg}^{2+}$  concentrations in the sediments, as the slopes of the models were  $-0.004 \pm 0.0003$  and  $0.46 \pm 0.01$  ( $t$ -value =  $-14.23$  and 47.12;  $p$ -value < 0.01) and the intercept values were  $2.91 \pm 0.11$  ( $t$ -value = 25.79;  $p$ -value < 0.001), respectively. However, the model for the Si concentrations did not produce viable results due to the nearly identical sediment concentration values obtained across the sampling sites (Figure 2).

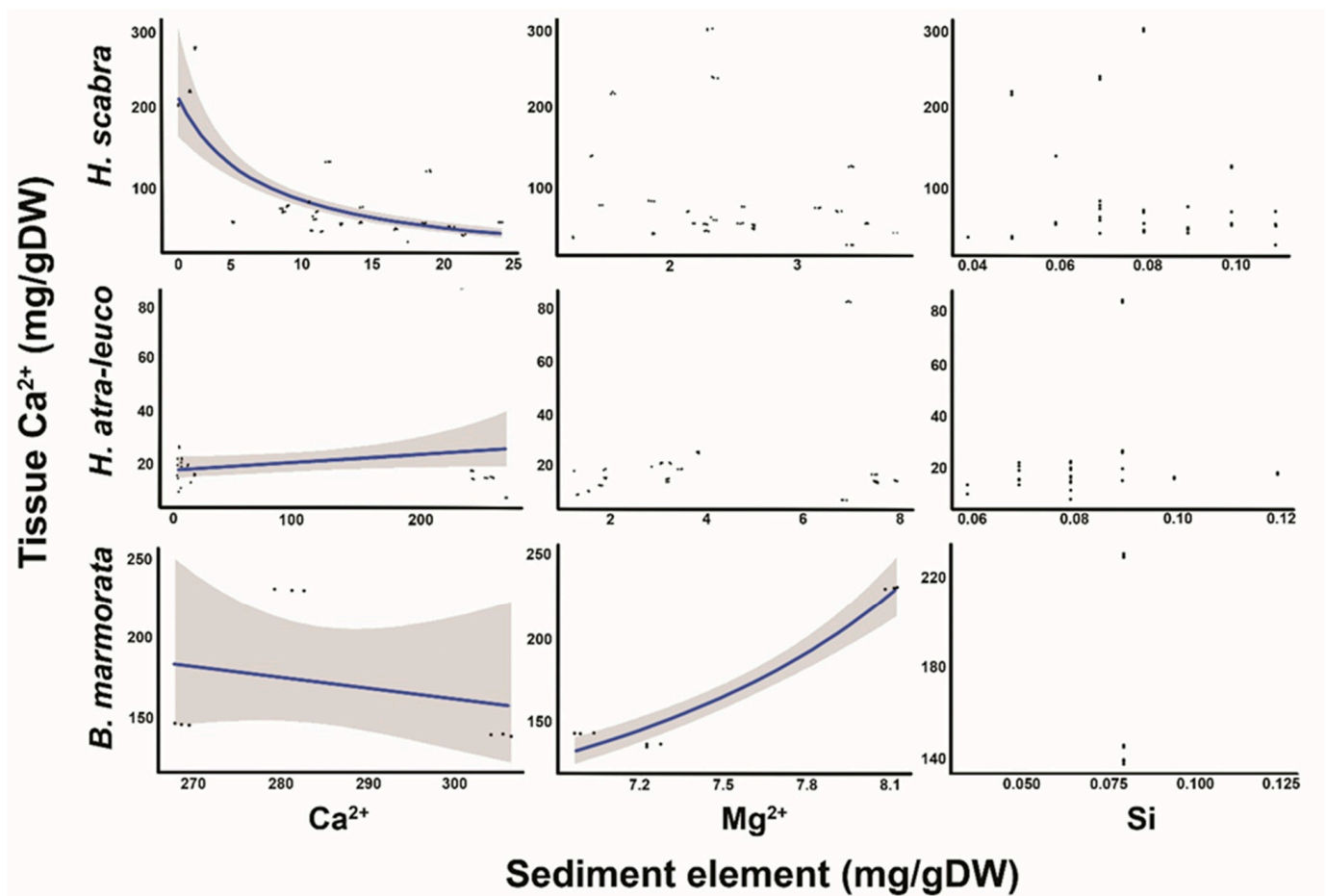


**Figure 2.** Relationship of  $\text{Ca}^{2+}$ ,  $\text{Mg}^{2+}$  and Si sediment concentrations, and  $\text{Ca}^{2+}$  concentrations in *H. scabra*, *H. atra-leucospilota* and *B. marmorata*. The line indicates a significant predictor, while the shaded areas represent a 95% CI.

### 3.3. Relationship between Tissue $\text{Mg}^{2+}$ and Sediment $\text{Ca}^{2+}$ , $\text{Mg}^{2+}$ and Si

The GLMM revealed that the  $\text{Ca}^{2+}$ ,  $\text{Mg}^{2+}$  and Si in the ambient sediment were significant predictors for the  $\text{Mg}^{2+}$  in the body walls of *H. scabra*, since the slopes of the models (log-scale) were  $-0.01 \pm 0.005$ ,  $-0.26 \pm 0.05$  and  $7.37 \pm 1.64$  (mean  $\pm$  SE;  $t$ -value =  $-2.11$ ,  $-5.41$  and  $4.48$ ;  $p$ -value  $< 0.05$ , Figure 3), and the intercept was  $3.10 \pm 0.11$  ( $t$ -value =  $27.05$ ;  $p$ -value  $< 0.001$ ). For *H. atra-leucospilota*, the GLMM revealed that the  $\text{Ca}^{2+}$ ,  $\text{Mg}^{2+}$  and Si in the ambient sediments did not significantly predict the  $\text{Mg}^{2+}$  in the body walls of *H. atra-leucospilota* (Figure 3). The GLM indicated that the  $\text{Mg}^{2+}$  concentrations in the body walls of *B. marmorata* could also be predicted by the  $\text{Ca}^{2+}$  and  $\text{Mg}^{2+}$  concentrations in the sediments, as the slopes of the models (log-scale) were  $-0.004 \pm 0.0002$  and  $0.18 \pm 0.01$  (mean  $t$ -value =  $-20.24$  and  $26.07$ ;  $p$ -value  $< 0.01$ ) and the intercept was  $2.70 \pm 0.10$  ( $t$ -value =  $34.9$ ;  $p$ -value  $< 0.001$ ). However, the model for the Si concentrations did not produce viable results due to the nearly identical sediment concentration values across the sampling sites (Figure 3).

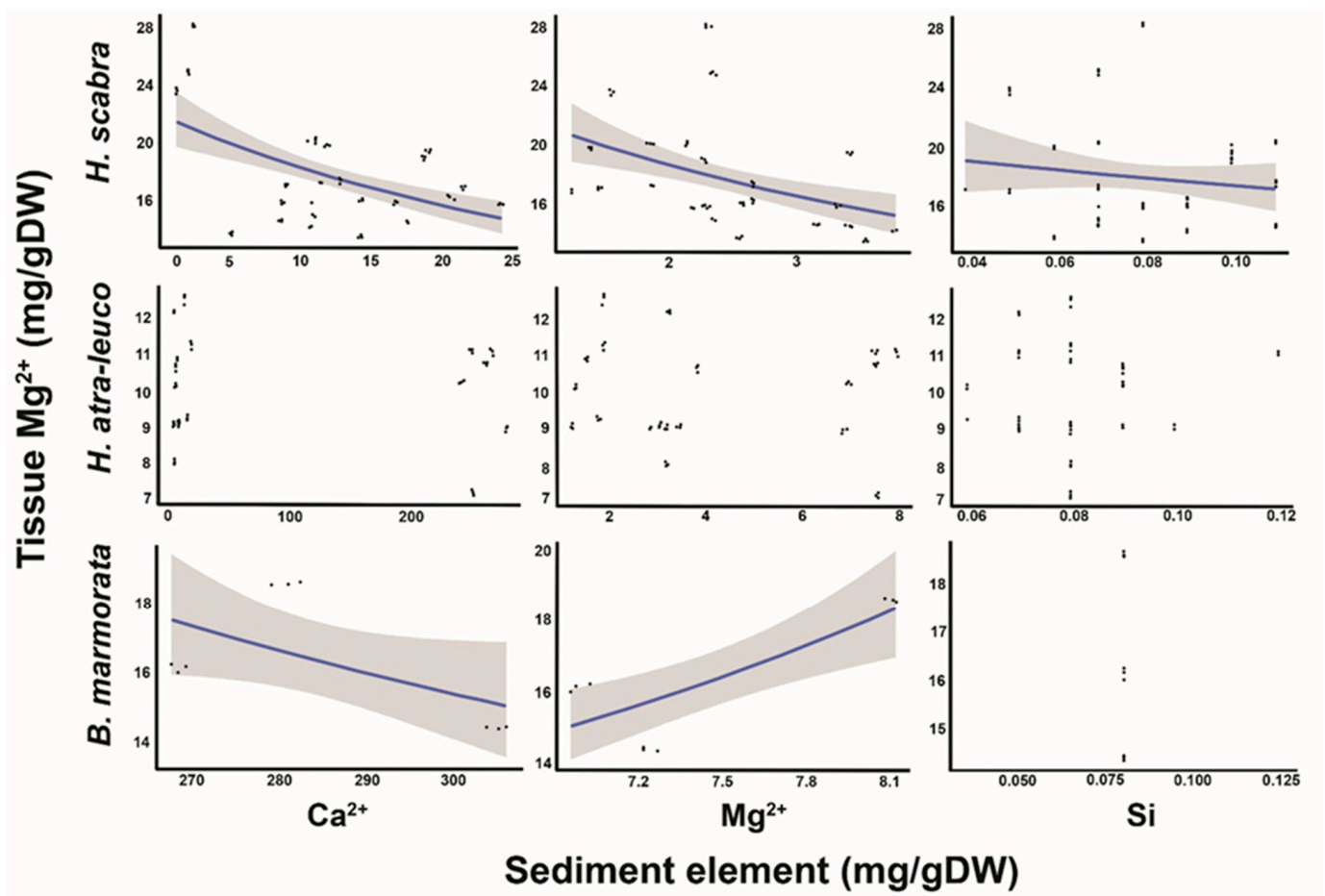


**Figure 3.** Relationship of  $\text{Ca}^{2+}$ ,  $\text{Mg}^{2+}$  and Si concentrations in the sediments to  $\text{Mg}^{2+}$  concentrations in the body walls of *H. scabra*, *H. atra-leucospilota* and *B. marmorata*. The line indicates a significant predictor, while the shaded areas represent a 95% CI.

### 3.4. Relationship between Tissue Si and Sediment $\text{Ca}^{2+}$ , $\text{Mg}^{2+}$ and Si

The GLMM revealed that the  $\text{Ca}^{2+}$  and  $\text{Mg}^{2+}$  in the ambient sediment were significant predictors for the Si in the body walls of *H. scabra*, where the slopes of the models (log-scale) were  $0.021 \pm 0.007$  and  $0.27 \pm 0.07$  (mean  $\pm$  SE;  $t$ -value = 2.93 and 4.09;  $p$ -value < 0.01, Figure 4), and the intercept was  $-3.85 \pm 0.19$  ( $t$ -value =  $-19.79$ ;  $p$ -value < 0.001). However, the Si in the body walls of *H. scabra* could not be predicted by the Si concentrations in the ambient sediment. For *H. atra-leucospilota*, the  $\text{Ca}^{2+}$  and  $\text{Mg}^{2+}$  in the ambient sediments did not predict the Si in the body walls of the sea cucumber (Figure 4). However, the Si in the sediment was a significant predictor for the Si in the body walls of *H. atra-leucospilota*, since the slope of the model (log-scale) was  $-15.0 \pm 6.1$  (mean  $\pm$  SE;  $t$ -value =  $-2.45$ ;  $p$ -value < 0.01) and the intercept was  $-2.71 \pm 0.52$  ( $t$ -value =  $-5.2$ ;  $p$ -value < 0.001). However, the model for the Si concentrations in the body walls of *B. marmorata* did not produce a viable result (Figure 4).

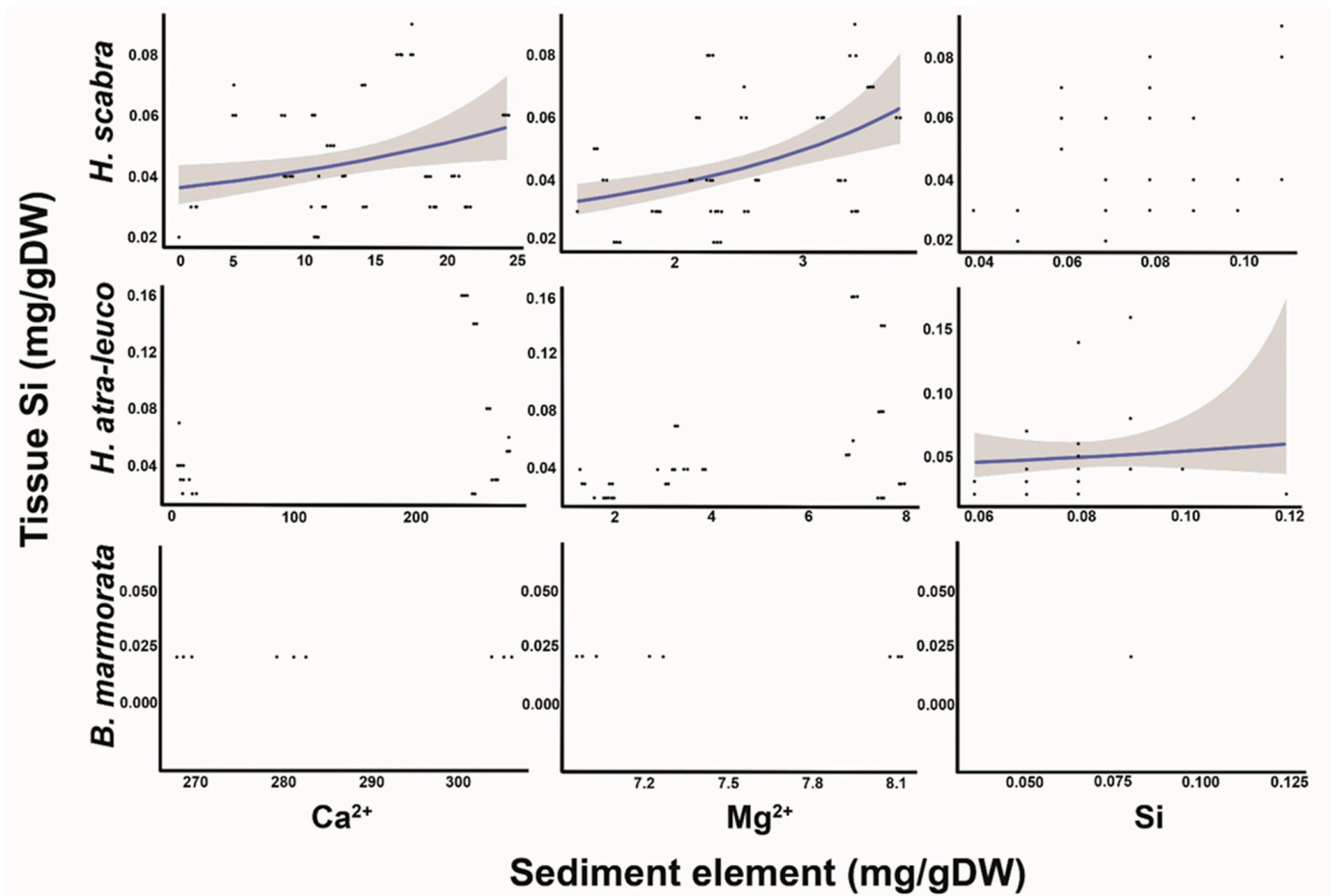


**Figure 4.** Relationship of the minerals  $\text{Ca}^{2+}$ ,  $\text{Mg}^{2+}$  and Si obtained from the sediments to the Si concentrations in the body walls of the sea cucumbers *H. scabra*, *H. atra-leucospilota* and *B. marmorata*. The line indicates the significant predictor, while the shaded area represents a 95% CI.

### 3.5. Relationship between Tissue Mg/Ca and Sediment $\text{Ca}^{2+}$ , $\text{Mg}^{2+}$ , Si and Mg/Ca

Exploring the relationship between the Mg/Ca ratio in the body walls and the  $\text{Ca}^{2+}$ ,  $\text{Mg}^{2+}$  and Si in the sediments using the GLMM revealed that, in *H. scabra*, the ratio was positively correlated to the  $\text{Ca}^{2+}$  concentrations in the sediments, but not to the  $\text{Mg}^{2+}$  and Si concentrations as observed in the slopes of the models (log-scale) and intercept values, which were  $0.04 \pm 0.006$  and  $-2.14 \pm 0.16$  (mean  $\pm$  SE;  $t$ -value = 6.49 and  $-13.13$ ;  $p$ -value  $\leq 0.01$ ), respectively (Figure 5). The Mg/Ca ratio in the body walls of *H. atra-leucospilota* increased as the  $\text{Ca}^{2+}$  concentrations increased in the sediments, and the reverse occurred for the  $\text{Mg}^{2+}$  since the slopes of the models (log-scale) were  $0.006 \pm 0.001$  and  $-0.27 \pm 0.07$  (mean  $\pm$  SE;  $t$ -value = 4.40 and  $-3.97$ ;  $p$ -value  $\leq 0.01$ ). For *B. marmorata*, the Mg/Ca ratio in the body walls was not significantly predicted by the  $\text{Ca}^{2+}$ , but was negatively correlated to the  $\text{Mg}^{2+}$  concentrations, and the GLM did not yield meaningful model results for the Si concentration since the slopes of the models were  $-0.28 \pm 0.07$  (mean  $\pm$  SE;  $t$ -value =  $-41.05$ ;  $p$ -value  $\leq 0.001$ ) (Figure 5). Additionally, the GLMM showed that the Mg/Ca in the body walls of *H. scabra* was negatively correlated to the Mg/Ca in the sediments, as the slope of the model was  $-0.974 \pm 0.096$  ( $t$ -value = 10.17;  $p$ -value  $< 0.01$ ) and the intercept was  $-1.116 \pm 0.044$  ( $t$ -value =  $-25.49$ ;  $p$ -value  $< 0.001$ ). For *H. atra-leucospilota*, the relationship between the Mg/Ca ratio in the body walls and the  $\text{Ca}^{2+}$ ,  $\text{Mg}^{2+}$  and Si in the sediments was not supported. The GLM model did not yield viable results for *B. marmorata*.

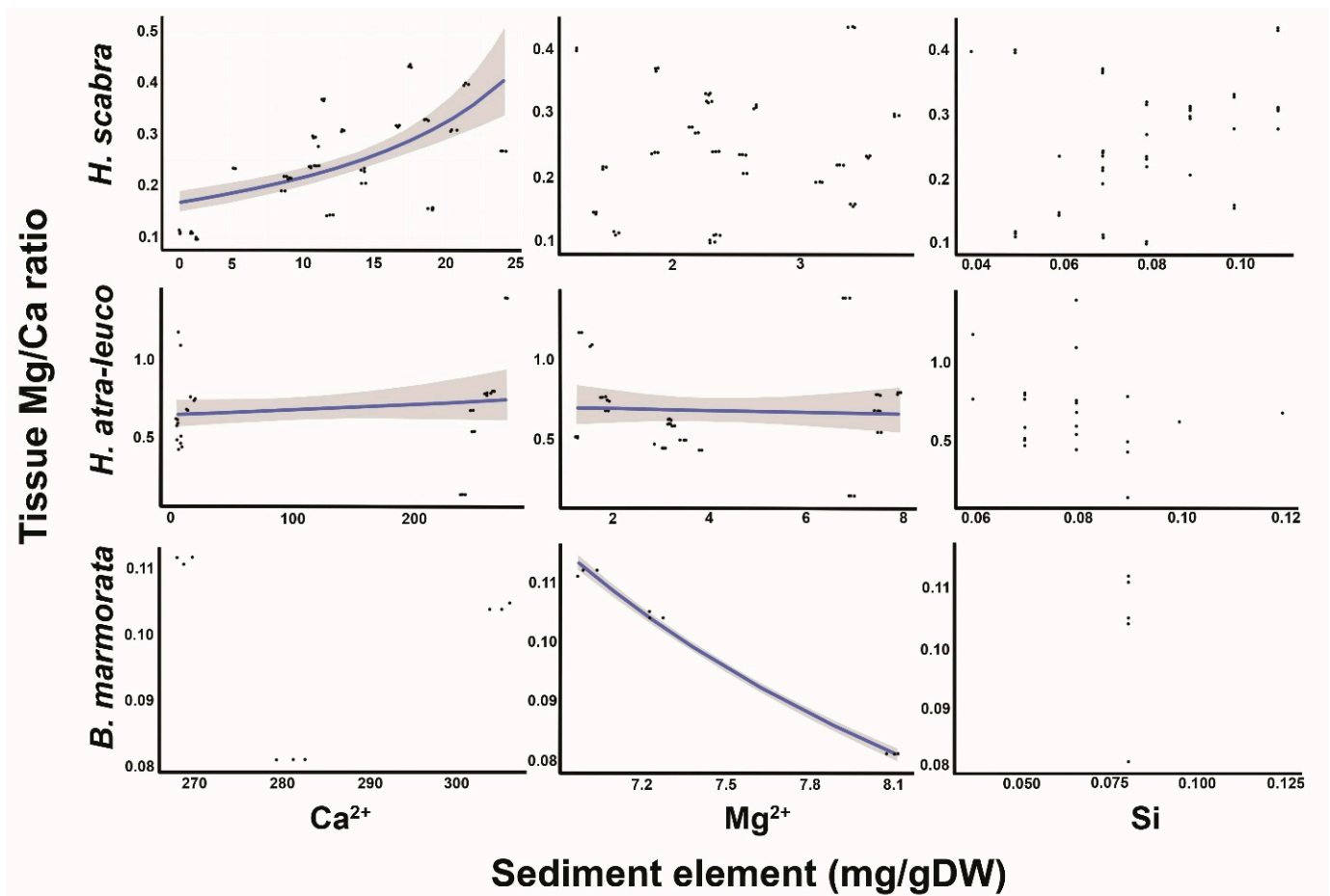


**Figure 5.** Relationship of the Mg:Ca ratio in the body walls of the sea cucumbers *H. scabra*, *H. atra-leucospilota* and *B. marmorata*, and the  $\text{Ca}^{2+}$ ,  $\text{Mg}^{2+}$  and Si concentrations in the sediments. The line indicates a significant predictor, while the shaded area represents a 95% CI.

#### 4. Discussion

##### 4.1. Comparison among Species and Locations

This study explored the relationship of the elements  $\text{Ca}^{2+}$ ,  $\text{Mg}^{2+}$  and Si between the sediments and the body walls of sea cucumbers in tropical seagrass meadows. The results suggested that the  $\text{Ca}^{2+}$  and  $\text{Mg}^{2+}$  concentrations in the body walls of sea cucumbers significantly vary according to species (Table 1). Furthermore, significant variations in the amount of these minerals in the sediments also varied with the locations, except Si, suggesting that the variation in the body walls could not be solely attributed to the physiology of sea cucumbers but also to the availability of minerals in the sediments and/or seawater. In the case of Si, the concentration of this mineral in the sediments did not vary with the location. This suggested that the potential accumulation of silicon in the sediments is likely due to eutrophication in coastal zones [20,45]. As a consequence, the concentration of Si was only significantly lower in *B. marmorata* compared to the rest of the species tested. The habitat of *B. marmorata* was a seagrass–coral reef site which is different from the rest of the habitats.

The possibility of contamination of the samples by the reagents is unlikely in the present study since the concentrations of silicon in both the sediment and body wall samples were above the detection limit of the ICP-OES machine. This means that the routine procedure of inter-elemental correction during measurements was effective at reducing the interferences from other elements and that the values obtained were from the samples and not from the contaminants. On the aspect concerning the close similarity of the  $\text{Mg}^{2+}$  concentrations in the body walls of *H. scabra*, regardless of the  $\text{Ca}^{2+}$  and  $\text{Mg}^{2+}$

concentrations in the sediment (Table 1), this result could not be solely interpreted in terms of the organism's response to the mineral content in the sediment. This is because many calcifying species are known to respond to a certain range of mineral concentrations, rather than to individual values (see [46–50]). It was emphasized that biological factors play an important role in controlling the magnesium content in echinoderm skeletons [17]. Nevertheless, seagrass meadows provided a suitable habitat for sea cucumbers, as well as in supplying minerals for metabolic activities and skeletal development.

#### 4.2. Relationship between Tissue $\text{Ca}^{2+}$ and Sediment $\text{Ca}^{2+}$ , $\text{Mg}^{2+}$ and Si

The relationship between the tissue  $\text{Ca}^{2+}$  and sediment  $\text{Ca}^{2+}$ ,  $\text{Mg}^{2+}$  and Si varied depending on the  $\text{Ca}^{2+}$  and  $\text{Mg}^{2+}$  content in the body walls of the sea cucumbers (Figure 2). Species that contain less calcium, such as *H. atra-leucospilota*, weakly responded to the availability of the  $\text{Ca}^{2+}$ ,  $\text{Mg}^{2+}$  and Si concentrations in the sediments, compared to *H. scabra* and *B. marmorata* which contain a high  $\text{Ca}^{2+}$  content (Figures 2–4). On the other hand, the sea cucumbers *H. scabra* and *B. marmorata* strongly responded to the changes in the mineral concentrations of the sediments due to the organism's great need for minerals. Such a response has been demonstrated in other calcifying organisms where an “open” or “closed” system of ion transport exists to enable species to respond to the availability of minerals in the seawater (e.g., [46–48]). Although the source of minerals for adult sea cucumbers is potentially derived from the seawater and/or sediment, essentially the same thermodynamic principle is at work in the biomineralization process, regardless of whether the source is obtained from the seawater or sediments.

#### 4.3. Relationship between Tissue $\text{Mg}^{2+}$ and Sediment $\text{Ca}^{2+}$ , $\text{Mg}^{2+}$ and Si

In terms of the  $\text{Mg}^{2+}$  content, *H. scabra* responded negatively to the increasing  $\text{Mg}^{2+}$  concentrations in the sediments, while a positive relationship was detected for *B. marmorata* (Figure 3). This indicates a species-specific response of the sea cucumbers to the increasing  $\text{Mg}^{2+}$  concentrations in the sediments. Additionally, although the  $\text{Mg}^{2+}$  concentration of *H. scabra* remained relatively unchanged between locations (i.e., Talibong and Muk Islands), regardless of the  $\text{Ca}^{2+}$  and  $\text{Mg}^{2+}$  contents, it is an indication that individuals belonging to the same species responded similarly to a certain range of mineral concentrations in the sediments. This result may have minimal implications to the findings that characterized the Mg–calcite composition of Antarctic echinoderms based on latitudes (i.e., [51]) and temperature variation [52]. Latitudinal and temperature differences cannot be implicated in the present study since the sampling sites were located just a few kilometers from each other with essentially a similar climate. Thus, the  $\text{Mg}^{2+}$  concentration in the sea cucumbers was characteristic for particular species and, thus, physiologically controlled with influence from the sediment and/or seawater mineralogy.

#### 4.4. Relationship between Tissue Si and Sediment $\text{Ca}^{2+}$ , $\text{Mg}^{2+}$ and Si

The relationship between the Si in the body walls of *H. scabra* and the  $\text{Ca}^{2+}$  and  $\text{Mg}^{2+}$  in the sediments was positive, except that the relationship with the Si in the sediment was not supported (Figure 4). We hypothesized that the Si molecules in the sediments were adsorbed to the calcium carbonates, which were then ingested by the sea cucumbers, but the small-sized Si were selectively disposed by way of the membrane transport system of the cells (i.e., [53,54]). Otherwise, the excess Si could affect the biomineralization process, leading to the alteration of the Mg/Ca ratio in the sea cucumbers. In the case of *H. atra-leucospilota*, it is discernible that this species is highly efficient at transporting ions across the cell membranes so that the  $\text{Ca}^{2+}$  and  $\text{Mg}^{2+}$  concentrations in the sediments are not associated to the Si concentration in the tissue. In the case of *B. marmorata*, the model did not give a meaningful result, probably due to the unique mineralogy and trophic interactions in the seagrass–coral reef habitat. Overall, the exact role of Si in sea cucumbers is not yet completely understood although this element has been widely implicated as a template for biomineralization.

#### 4.5. Relationship between Tissue Mg:Ca Ratio and Sediment $\text{Ca}^{2+}$ , $\text{Mg}^{2+}$ and Si

A strong positive association between the Mg/Ca in the body walls of *H. Scabra* and the  $\text{Ca}^{2+}$  content in the sediments was detected, although there was no relationship with the  $\text{Mg}^{2+}$  and Si (Figure 5). The correlation was similar to those observed in other marine calcifying organisms where changes in the concentration of  $\text{Ca}^{2+}$  and Mg/Ca in the seawater influenced the precipitation of nonskeletal carbonates, such that a low-Mg calcite was formed when the ambient Mg:Ca molar ratio was  $<1$  (e.g., [46–48]). In the case of *H. atra-leucospilota*, there were weak associations between the tissue Mg/Ca and  $\text{Ca}^{2+}$  and  $\text{Mg}^{2+}$  in the sediments, which again demonstrates the strong biological exclusion mechanism of this species. In the case of *B. marmorata*, the model did not produce meaningful results, except for  $\text{Mg}^{2+}$ , potentially due to the unique mineralogy of the seagrass–coral reef landscape. Overall, the biomineralization occurring in echinoderms is under the control of secretory cells (i.e., soft tissues), which prevent the build-up of excess  $\text{Ca}^{2+}$  during calcium carbonate precipitation [5,49,50].

## 5. Conclusions

This study provided a basic understanding of the interrelationship of the elements  $\text{Ca}^{2+}$ ,  $\text{Mg}^{2+}$  and Si between the sediments and body walls of sea cucumbers in tropical seagrass meadows. We observed that the concentrations of the minerals  $\text{Ca}^{2+}$  and  $\text{Mg}^{2+}$  in the body walls of sea cucumbers varied according to species, with *H. scabra* and *B. marmorata* containing a higher  $\text{Ca}^{2+}$  content compared to *H. atra* and *H. leucospilota*. In contrast, the Si concentration did not vary with the locations nor in terms of the species, except only for *B. marmorata* whose habitat is a seagrass–coral reef site. Generally, the mineral concentration in the body walls of *H. scabra* and *B. marmorata* showed a stronger association with the sediment mineralogy as compared to that of the *H. atra-leucospilota*. It may be implied that the former two species have a weaker biological control of biomineralization as compared to the latter, thus making *H. scabra* and *B. marmorata* vulnerable to climatic changes. However, our findings are preliminary and require further research as the sea cucumber's responses to sediment mineralogy vary considerably. It is, therefore, crucial to conduct a rigorous study to determine the application of the present results in order to address the declining sea cucumber population due to eutrophication.

**Author Contributions:** Conceptualization, A.F.; methodology, A.F., P.T. and A.P.; statistical analysis and visualization, P.T.; resources, A.F., A.P and K.-i.H.; writing—original draft preparation, A.F. and P.T.; writing—review and editing, K.-i.H., P.T. and A.P.; supervision, A.P. All the authors contributed to the article and approved the submitted version. All authors have read and agreed to the published version of the manuscript.

**Funding:** This research was partially supported by the JSPS Core-to-Core Program CREPSUM JPJSCCB20200009, the emergence of Skin Ulceration Diseases in Edible Sea Cucumbers in a Global Change Framework grant no. P-18-50965, the Center of Excellence on Biodiversity (BDC), Office of Higher Education Commission, grant no. BDC-PG3-160017 and Kitasato University Grant for International Exchange Programme.

**Institutional Review Board Statement:** The license to use animals for scientific purposes, ID U1-07888-2561, dated 12 February 2019, was provided by the Institute of Animals for Scientific Purpose Development (IAD), National Research Council of Thailand (NRCT).

**Informed Consent Statement:** Not applicable.

**Data Availability Statement:** Not applicable.

**Acknowledgments:** We would like to acknowledge J. Panyawan for the assistance in processing the samples. Thanks are owed to S. Puchakarn for the species identification of our specimens. Special thanks to P. Cadiz, A. Maypa, CE Nuevo and A. Tiongson for their comments on the manuscript. The support provided by the SSRU Graduate School of PSU and Silliman University is gratefully acknowledged. This research was supported by the Higher Education Research Promotion and Thailand's Education Hub for the Southern Region of ASEAN countries Project Office of the Higher Education Commission. This work was part of a Ph.D thesis in the Department of Biology, Division of Biological Science, Faculty of Science, Prince of Songkla University, Thailand for A.S.F, and partially supported by FDA-CO-2561-7938-TH.

**Conflicts of Interest:** The authors declare no conflict of interest.

## References

1. Guerrero, A.; Rodríguez Forero, A. Histological characterization of skin and radial bodies of two species of genus *Isostichopus* (Echinodermata: Holothuroidea). *Egypt. J. Aquat. Res.* **2018**, *44*, 155–161. [\[CrossRef\]](#)
2. Takemae, N.; Nakaya, F.; Motokawa, T. Low oxygen consumption and high body content of catch connective tissue contribute to low metabolic rate of sea cucumbers. *Biol. Bull.* **2009**, *216*, 45–54. [\[CrossRef\]](#) [\[PubMed\]](#)
3. Candia Carnevali, M.D. Regenerative response and endocrine disrupters in crinoid echinoderms: An old experimental model, a new ecotoxicological test. *Prog. Mol. Subcell. Biol.* **2005**, *39*, 167–200. [\[CrossRef\]](#) [\[PubMed\]](#)
4. Inoue, M.; Tamori, M.; Motokawa, T. Innervation of holothurian body wall muscle: Inhibitory effects and localization of 5-HT. *Zool. Sci.* **2002**, *19*, 1217–1222. [\[CrossRef\]](#)
5. Matsuno, A.; Motokawa, T. Evidence for calcium translocation in catch connective tissue of the sea cucumber *Stichopus chloronotus*. *Cell Tissue Res.* **1992**, *267*, 307–312. [\[CrossRef\]](#)
6. Hayashi, Y.; Motokawa, T. Effects of ionic environment on viscosity of catch connective tissue in Holothurian body wall. *J. Exp. Biol.* **1986**, *125*, 71–84. [\[CrossRef\]](#)
7. Ries, J.B. Review: Geological and experimental evidence for secular variation in seawater Mg/Ca (calcite-aragonite seas) and its effects on marine biological calcification. *Biogeosciences* **2010**, *7*, 2795–2849. [\[CrossRef\]](#)
8. Marin, F.; Bundeleva, I.; Takeuchi, T.; Immel, F.; Medakovic, D. Organic matrices in metazoan calcium carbonate skeletons: Composition, functions, evolution. *J. Struct. Biol.* **2016**, *196*, 98–106. [\[CrossRef\]](#)
9. Clark, M.S. Molecular mechanisms of biomineralization in marine invertebrates. *J. Exp. Biol.* **2020**, *223*, jeb206961. [\[CrossRef\]](#)
10. Sun, N.; Wu, H.; Du, M.; Tang, Y.; Liu, H.; Fu, Y.; Zhu, B. Food protein-derived calcium chelating peptides: A review. *Trends Food Sci. Technol.* **2006**, *58*, 140–148. [\[CrossRef\]](#)
11. Vrieling, E.G.; Beelen, T.P.M.; Sun, Q.; Hazelaar, S.; van Santen, R.A.; Gieskes, W.W.C. Ultrasmall, Small, and Wide Angle X-ray Scattering analysis of diatom biosilica: Interspecific differences in fractal properties. *J. Mater. Chem.* **2004**, *14*, 1970–1975. [\[CrossRef\]](#)
12. Rondanelli, M.; Faliva, M.A.; Peroni, G.; Gasparri, C.; Perna, S.; Riva, A.; Petrangolini, G.; Tartara, A. Silicon: A neglected micronutrient essential for bone health. *Exp. Biol. Med.* **2021**, *246*, 1500–1511. [\[CrossRef\]](#) [\[PubMed\]](#)
13. Jugdaohsingh, R. Silicon and bone health. *J. Nutr. Health Aging* **2007**, *11*, 99–110, PMID:PMC2658806. [\[PubMed\]](#)
14. Ziola-Frankowska, A.; Kubaszewski, Ł.; Dąbrowski, M.; Frankowski, M. Interrelationship between silicon, aluminum, and elements associated with tissue metabolism and degenerative processes in degenerated human intervertebral disc tissue. *Environ. Sci. Pollut. Res.* **2017**, *24*, 19777–19784. [\[CrossRef\]](#)
15. Lowenstam, H.A.; Rossman, G.R. Amorphous, hydrous, ferric phosphatic dermal granules in *Molpadia* (Holothuroidea): Physical and chemical characterization and ecologic implications of the bioinorganic fraction. *Chem. Geol.* **1975**, *15*, 15–51. [\[CrossRef\]](#)
16. Barzkar, N.; Fariman, G.A.; Taheri, A. Proximate composition and mineral contents in the body wall of two species of sea cucumber from Oman Sea. *Environ. Sci. Pollut. Res.* **2017**, *24*, 18907–18911. [\[CrossRef\]](#)
17. Iglukowska, A.; Najorka, J.; Voronkov, A.; Chelchowski, M.; Kuklinski, P. Variability in magnesium content in Arctic echinoderm skeletons. *Mar. Environ. Res.* **2017**, *129*, 207–218. [\[CrossRef\]](#)
18. Thomson, T. Silicon. In *Methods in Geochemistry and Geophysics*; Easton, A.J., Ed.; Elsevier Publishing Company: Amsterdam, The Netherlands, 1972; Volume 6, pp. 71–94. [\[CrossRef\]](#)
19. Kumar, S.; Natalio, F.; Elbaum, R. Protein-driven biomineralization: Comparing silica formation in grass silica cells to other biomineralization processes. *J. Struct. Biol.* **2021**, *213*, 107665. [\[CrossRef\]](#)
20. Conley, D.J.; Chelske, C.L.; Stoermer, E.F. Modification of the biogeochemical cycle of silica with eutrophication. *Mar. Ecol. Prog. Ser.* **1993**, *101*, 179–192. [\[CrossRef\]](#)
21. Tambutté, S.; Holcomb, M.; Ferrier-Pagès, C.; Reynaud, S.; Tambutté, É.; Zoccola, D.; Allemand, D. Coral biomineralization: From the gene to the environment. *J. Exp. Mar. Biol. Ecol.* **2011**, *408*, 58–78. [\[CrossRef\]](#)
22. Smith, A.B. Echinoderm Larvae and Phylogeny. *Annu. Rev. Ecol. Syst.* **1997**, *28*, 219–241. [\[CrossRef\]](#)
23. Hammond, L.S. An analysis of grain size modification in biogenic carbonate sediments by deposit-feeding holothurians and echinoids. *Limnol. Oceanogr.* **1981**, *26*, 898–906. [\[CrossRef\]](#)

24. Schneider, K.; Silverman, J.; Kravitz, B.; Rivlin, T.; Schneider-Mor, A.; Barbosa, S.; Byrne, M.; Caldeira, K. Inorganic carbon turnover caused by digestion of carbonate sands and metabolic activity of holothurians. *Estuar. Coast. Shelf Sci.* **2013**, *133*, 217–223. [[CrossRef](#)]
25. Floren, A.S.; Hayashizaki, K.I.; Tuntiprapas, P.; Prathep, A. Contributions of seagrasses and other sources to sea cucumber diets in a tropical seagrass ecosystem. *Chiang Mai J. Sci.* **2021**, *48*, 1259–1270.
26. Yuan, X.; McCoy, S.J.; Du, Y.; Widdicombe, S.; Hall-Spencer, J.M. Physiological and behavioral plasticity of the sea cucumber *Holothuria forskali* (Echinodermata, Holothuroidea) to acidified seawater. *Front. Physiol.* **2018**, *9*, 1–10. [[CrossRef](#)]
27. Chen, Z.; Mayer, L.M.; Weston, D.P.; Bock, M.J.; Jumars, P.A. Inhibition of digestive enzyme activities by copper in the guts of various marine benthic invertebrates. *Environ. Toxicol. Chem.* **2002**, *21*, 1243–1248. [[CrossRef](#)]
28. Dickson, J.A.D. Fossil echinoderms as monitor of the Mg/Ca ratio of Phanerozoic oceans. *Science* **2002**, *298*, 1222–1224. [[CrossRef](#)]
29. Stanley, S.M. Influence of seawater chemistry on biomineralization throughout phanerozoic time: Paleontological and experimental evidence. *Palaeogeogr. Palaeoclimatol. Palaeoecol.* **2006**, *232*, 214–236. [[CrossRef](#)]
30. Asnaghi, V.; Mangialajo, L.; Gattuso, J.-P.; Francour, P.; Privitera, D.; Chiantore, M. Effects of ocean acidification and diet on thickness and carbonate elemental composition of the test of juvenile sea urchins. *Mar. Environ. Res.* **2014**, *93*, 78–84. [[CrossRef](#)]
31. Kořbuk, D.; Dubois, P.; Stolarski, J.; Gorzelak, P. Effects of seawater chemistry (Mg<sup>2+</sup>/Ca<sup>2+</sup> ratio) and diet on the skeletal Mg/Ca ratio in the common sea urchin *Paracentrotus lividus*. *Mar. Environ. Res.* **2019**, *145*, 22–26. [[CrossRef](#)]
32. Ricart, A.M.; Dalmau, A.; Perez, M.; Romero, J. Effects of landscape configuration on the exchange of materials in seagrass ecosystems. *Mar. Ecol. Prog. Ser.* **2015**, *532*, 89–100. [[CrossRef](#)]
33. Belbachir, N.E.; Lepoint, G.; Mezali, K. Comparison of isotopic niches of four sea cucumbers species (Holothuroidea: Echinodermata) inhabiting two seagrass meadows in the southwestern Mediterranean Sea (Mostaganem, Algeria). *Belgian J. Zool.* **2019**, *149*, 95–106. [[CrossRef](#)]
34. Khogkhao, C.; Hayashizaki, K.I.; Tuntiprapas, P.; Prathep, A. Changes in seagrass communities along the runoff gradient of the Trang river, Thailand. *ScienceAsia* **2017**, *43*, 339–346. [[CrossRef](#)]
35. Rattanachot, E.; Prathep, A. Temporal variation in growth and reproduction of *Enhalus acoroides* (L. f.) Royle in a monospecific meadow in Haad Chao Mai National Park, Trang Temporal variation in growth and reproduction of *Enhalus acoroides* (L. f.) Royle in a monospecific meadow. *Bot. Mar.* **2015**, *54*, 201–207. [[CrossRef](#)]
36. Rattanachot, E. Effect of Shoot Density on Growth, Recruitment and Reproduction of *Enhalus acoroides* (L.f.) Royle at Haad Chao Mai National Park, Trang Province, Thailand. Master's Thesis, Prince of Songkla University, Songkla, Thailand, 2008.
37. Floren, A.; Hayashizaki, K.I.; Puchakarn, S.; Tuntiprapas, P.; Prathep, A. A Review of Factors Influencing the Seagrass-Sea Cucumber Association in Tropical Seagrass Meadows. *Front. Mar. Sci.* **2021**, *8*, 696134. [[CrossRef](#)]
38. Warnau, M.; Dutrieux, S.; Dúbois, P.; Ledent, G.; Rodriguez y Baena, A.M. Heavy metals in the sea cucumber *Holothuria tubulosa* (echinodermata) from the mediterranean *Posidonia oceanica* ecosystem: Body compartment, seasonal, geographical and bathymetric variations. *Environ. Bioindic.* **2006**, *1*, 268–285. [[CrossRef](#)]
39. Turk Culha, S.; Dereli, H.; Karaduman, F.R.; Culha, M. Assessment of trace metal contamination in the sea cucumber (*Holothuria tubulosa*) and sediments from the Dardanelles Strait (Turkey). *Environ. Sci. Pollut. Res.* **2016**, *23*, 11584–11597. [[CrossRef](#)]
40. R Core Team. *R: A Language and Environment for Statistical Computing*; R Foundation for Statistical Computing: Vienna, Austria, 2021. Available online: <https://www.R-project.org> (accessed on 8 December 2021).
41. Mangiafico, S. Rcompanion: Functions to Support Extension Education Program Evaluation. R Package Version 2.4.1. 2021. Available online: <https://CRAN.R-project.org/package=rcompanion> (accessed on 8 December 2021).
42. Ogle, D.H.; Wheeler, P.; Dinno, A. FSA: Fisheries Stock Analysis. R Package Version 0.8.32. 2021. Available online: <https://github.com/droglenc/FSA> (accessed on 8 December 2021).
43. Venables, W.N.; Ripley, B.D. *Modern Applied Statistics*, 4th ed.; Springer: New York, NY, USA, 2002; ISBN 0-387-95457-0.
44. Bates, D.; Maechler, M.; Bolker, B.; Walker, S. Fitting Linear Mixed-Effects Models Using lme4. *J. Stat. Softw.* **2015**, *67*, 1–48. [[CrossRef](#)]
45. Duarte, C.M. Submerged aquatic vegetation in relation to different nutrient regimes. *Ophelia* **1995**, *41*, 87–112. [[CrossRef](#)]
46. Ries, J.B. Effect of ambient Mg/Ca ratio on Mg fractionation in calcareous marine invertebrates: A record of the oceanic Mg/Ca ratio over the Phanerozoic. *Geology* **2004**, *32*, 981–984. [[CrossRef](#)]
47. Ries, J.B. Aragonite production in calcite seas: Effect of seawater Mg/Ca ratio on the calcification and growth of the calcareous alga *Penicillus capitatus*. *Paleobiology* **2005**, *31*, 445–458. [[CrossRef](#)]
48. Stanley, S.M.; Ries, J.B.; Hardie, L.A. Seawater chemistry, coccolithophore population growth, and the origin of Cretaceous chalk. *Geology* **2005**, *33*, 593–596. [[CrossRef](#)]
49. Simkiss, K.; Wilbur, K.M. *Biomineralization: Cell Biology and Mineral Deposition*, 1st ed.; Academic Press: San Diego, CA, USA, 1989.
50. Chan, N.C.S.; Connolly, S.R. Sensitivity of coral calcification to ocean acidification: A meta-analysis. *Glob. Change Biol.* **2013**, *19*, 282–290. [[CrossRef](#)]
51. McClintock, J.B.; Amsler, M.O.; Angus, R.A.; Challener, R.C.; Schram, J.B.; Amsler, C.D.; Mah, C.L.; Cuce, J.; Baker, B.J. The Mg-calcite composition of Antarctic echinoderms: Important implications for predicting the impacts of ocean acidification. *J. Geol.* **2011**, *119*, 457–466. [[CrossRef](#)]

52. Hermans, J.; Borremans, C.; Willenz, P.; André, L.; Dubois, P. Temperature, salinity and growth rate dependences of Mg/Ca and Sr/Ca ratios of the skeleton of the sea urchin *Paracentrotus lividus* (Lamarck): An experimental approach. *Mar. Biol.* **2010**, *157*, 1293–1300. [[CrossRef](#)]
53. Carafoli, E. Intracellular calcium homeostasis. *Ann. Rev. Biochem.* **1987**, *56*, 395–433. [[CrossRef](#)]
54. Yeagle, P. *The Membrane of Cells*, 3rd ed.; Academic Press: Cambridge, MA, USA, 2016; pp. 335–378.

**Disclaimer/Publisher’s Note:** The statements, opinions and data contained in all publications are solely those of the individual author(s) and contributor(s) and not of MDPI and/or the editor(s). MDPI and/or the editor(s) disclaim responsibility for any injury to people or property resulting from any ideas, methods, instructions or products referred to in the content.